Molecular Dynamics of the Anti-Fluorescein 4−4−20 Antigen-Binding Fragment. 2. Time-Resolved Fluorescence Spectroscopy†

Kap Lim,‡,§ David M. Jameson,‖ Christine A. Gentry,‡ and James N. Herron*,‡

Departments of Pharmaceutics and Bioengineering, University of Utah, Salt Lake City, Utah 84112, and Department of Biochemistry and Biophysics, John A. Burns School of Medicine, University of Hawaii, Honolulu, Hawaii 96822

Received September 21, 1994; Revised Manuscript Received February 28, 1995⊗

ABSTRACT: Time-resolved fluorescence experiments were performed to investigate the dynamic aspects of the antigen-binding fragment (Fab) of a high-affinity monoclonal antibody (4−4−20) which binds the fluorescent hapten fluorescein. Both the unliganded Fab and a complex of the Fab with a nonfluorescent analog of fluorescein (fluoresceinamine, FLM) were examined. A fluorescence polarization probe [5-[[2-[(iodoacetyl)amino]ethyl]amino]naphthalene-1-sulfonic acid, AEDANS] was covalently attached to the C-terminus of the Fab. Experiments were performed at three different temperatures (10, 25, and 35 °C), and phase-modulation data sets were collected for five different molar ratios of FLM to Fab at each temperature. Global analyses were then used to extract values for fluorescence lifetime and rotational correlation time from these data. In the lifetime analysis the best fit was obtained when the emission of AEDANS was described by a Lorentzian distribution of lifetimes (τ = 15.6 ns, distribution width = 3.4 ns, both at 25 °C), which suggested that the probe experienced a heterogeneous environment. Anisotropy analyses suggested that two different rotational components were present. The first was attributed to the global motion of the Fab and exhibited a rotational correlation time (θ_1) of *ca.* 33 ns at 25 °C. This component was relatively unaffected by antigen binding. The second rotational component was attributed to the local or segmental motion within the Fab and exhibited a rotational correlation time (θ_2) of 1.1 ns at 25 °C. This value increased by more than 50% upon antigen binding, a result which was consistent with molecular dynamics simulations of the same Fab−fluorescein system [Lim & Herron (1995) *Biochemistry 34*, 6962−6974]. Furthermore, statistical analysis showed that this increase was significant at the 95% confidence level.

An immunoglobulin molecule consists of 12 closely interacting domains which are organized into three functional units—two identical antigen-binding fragments (Fab)[1] and a single constant fragment (Fc). The amino acid sequence of the N-terminal region of the Fab is highly variable in order to allow combination with a large number of antigenic determinants or epitopes. The Fc is structurally conserved in order to trigger immune effector functions common to many types of antibody molecules. Each Fab fragment is connected to the Fc via an extended polypeptide region (*ca.* 15 amino acids) which is called the hinge region.

The hydrodynamic behavior of immunoglobulins and their fragments has been investigated for more than 20 years using techniques such as fluorescence anisotropy and electron spin resonance (Cathou, 1978; Nezlin, 1990). Of particular interest has been a series of studies in which the antigen itself was used as a fluorescent or spin-label probe. The earliest of these was a study of polyclonal anti-dansyl antibodies by Yguerabide *et al.* (1970), which suggested that global rotation of the entire IgG and segmental flexibility at the hinge region constituted the major motions of the antibody molecule. However, a more careful analysis by Hanson *et al.* (1981, 1985) suggested that the longer rotational correlation time, previously thought to be due to the tumbling of the whole antibody, may arise instead from nearly independent motions of the Fab and Fc regions. This hypothesis was investigated further by Oi *et al.* (1983), who used mouse monoclonal anti-dansyl antibodies with the same light chain and variable heavy domain but with different heavy chain constant domains. They observed that values for the mean rotational correlation time for intact antibodies were variable, but those for Fab fragments were nearly identical. These differential flexibilities were shown to correlate to the ability of antibodies to fix the complement proteins. Pilz *et al.* (1973, 1975) studied the hydrodynamic properties of polyclonal anti-poly(D-alanyl) antibodies by small-angle X-ray scattering. They found that whereas the

† This work was supported in part by USPHS Grant AI 22898 and the Center for Biopolymers at Interfaces at the University of Utah.

‡ University of Utah.

§ Present address: ES 76 Biophysics Branch, George C. Marshall Space Flight Center, NASA, Huntsville, AL 35812.

‖ University of Hawaii.

⊗ Abstract published in *Advance ACS Abstracts,* May 1, 1995.

[1] Abbreviations: 4−4−20, high-affinity murine monoclonal anti-fluorescein antibody; AEDANS, 5-[[2-(acetylamino)ethyl]amino]naphthalene-1-sulfonic acid (when conjugated to a protein); ac, alternating current; Arg, arginine; C_H1, first constant domain of the immunoglobulin heavy chain; C_L, constant domain of the immunoglobulin light chain; Cys, cysteine; DEAE, diethylaminoethyl; DTT, dithiothreitol; EDTA, ethylenediaminetetraacetic acid; Fab, antigen-binding fragment; Fab′, antigen-binding fragment with cysteine group(s) near the C-terminus; $F(ab')_2$, two Fab′ fragments connected by one or more disulfide bonds; Fab−AEDANS, AEDANS conjugated to an antigen-binding fragment; Fc, constant fragment; FLM, fluoresceinamine (5-aminofluorescein); Glu, glutamic acid; Gly, glycine; 1,5-IAEDANS, 5-[[2-[(iodoacetyl)-amino]ethyl]amino]naphthalene-1-sulfonic acid (reactive form of AEDANS); IgG, immunoglobulin G; Ile, isoleucine; Lys, lysine; MD, molecular dynamics; MW, molecular weight; ND-PAGE, nondenaturing polyacrylamide gel electrophoresis; Pro, proline; r_0, limiting anisotropy; SDS−PAGE, sodium dodecyl sulfate−polyacrylamide gel electrophoresis; τ, fluorescence lifetime; θ, rotational correlation time; UV, ultraviolet; χ^2, chi-squared.

0006-2960/95/0434-6975$09.00/0

radius of gyration and volume of the intact antibody changed upon binding of the antigen, the radii of the $F(ab')_2$ and Fab' fragments did not. Finally, a neutron scattering study by Sosnick *et al.* (1992) showed that there was a distribution of distances between the antigen-binding sites of the two Fab fragments in an intact IgG antibody, indicating a high degree of flexibility of the Fab arms.

Although segmental flexibility of immunoglobulin molecules has clearly been demonstrated at the level of the Fab and Fc fragments, due consideration has not been given to segmental motions which may occur within these fragments. In our preceding paper (Lim & Herron, 1995) molecular dynamics (MD) simulations were performed in parallel for the Fab of a high affinity anti-fluorescein antibody (4−4−20) both with and without fluorescein bound to the antigen-combining site. These simulations strongly suggested that vibrational and rotational motions of the Fab were more correlated in the liganded state than in the unliganded state. Furthermore, quaternary structural differences were observed between the Fab with and without fluorescein, and in the former, fluorescein behaved as if it were an integral part of the Fab fragment.

In this paper, we use time-resolved fluorescence spectroscopy to examine the predictions of our MD simulations. A fluorescent probe was attached to the 4−4−20 Fab at its C-terminus using site-specific conjugation chemistry. Frequency domain time-resolved experiments were performed to measure the lifetimes and rotational modalities of labeled Fab fragments—both with and without antigen. Also, steady-state anisotropy measurements were conducted to complement the time-resolved fluorescence experiments.

MATERIALS AND METHODS

Preparation of the $F(ab')_2$ Fragments. The hybridoma cell line for 4−4−20 (Kranz & Voss, 1981a) was obtained from Prof. E. W. Voss, Jr. (University of Illinois at Urbana-Champaign). The 4−4−20 antibody was produced in BALB/c mice and purified as described by Herron *et al.* (1994). The purified antibody was digested with pepsin to produce $F(ab')_2$ fragments as described by Parham (1983). Specifically, *ca.* 30 mg of antibody (3−5 mg/mL) was dialyzed into 0.1 M sodium acetate buffer (pH 4.2), and then pepsin (Sigma Chemicals, St. Louis, MO) was added at a ratio of 1 mg of pepsin per 15 mg of IgG. This solution was incubated in a water bath at 37 °C for 8 h. The reaction was terminated by increasing the pH to 7.5 using 2 M Tris-HCl buffer (pH 8.8). Next, $F(ab')_2$ fragments were purified by FPLC with the following two steps: (i) size exclusion chromatography using a Superdex 200 Hiload column (Pharmacia) equilibrated in 50 mM diethanolamine buffer, pH 9.4, and (ii) chromatofocusing with a Mono P column (Pharmacia) in a pH gradient from 9 to 8.

Fluorescent Labeling of the Fab'. Fab' fragments with reactive thiol groups were prepared from the reduction of $F(ab')_2$ fragments with dithiothreitol (DTT) (Sigma Chemicals) and then labeled with 5-[[2-[(iodoacetyl)amino]ethyl]-amino]naphthalene-1-sulfonic acid (1,5-IAEDANS) (Molecular Probes, Eugene, OR). The following reagents were added to a 1 mL solution of 1 mg/mL $F(ab')_2$: 0.22 mL of 1 M Tris-HCl, pH 7.37; 22 μL of 0.2 M EDTA; and 13 μL of 0.1 M DTT dissolved in the Tris-HCl buffer. The final concentration of DTT in the reaction mixture was 1 mM. After reaction for 45 min at room temperature, the solution was passed through a PD-10 column (Pharmacia) equilibrated in 0.1 M sodium phosphate buffer (pH 8), which contained 5 mM EDTA. The Fab' fractions were combined and reacted with 1,5-IAEDANS. The mole ratio of 1,5-IAEDANS to Fab' in the reaction mixture was 1.2:1. The labeling reaction was allowed to proceed for 5 h at room temperature in the dark. The reaction was terminated by addition of iodoacetamide to prevent oxidation of Fab' fragments back into $F(ab')_2$ fragments. The Fab-AEDANS conjugate was purified using a PD-10 column equilibrated in 0.1 M sodium phosphate buffer, pH 8.0. This buffer was also used in all subsequent fluorescence measurements. The concentration of the Fab' fragments was determined by UV absorption measurement at 278 nm using an extinction coefficient of 1.5 mL mg^{-1} cm^{-1}. A molecular weight of 48 000 was used for the Fab', a value based on its amino acid sequence. The degree of labeling of the Fab' fragments labeled with AEDANS was determined by UV absorbance at 337 nm using an extinction coefficient of 6100 M^{-1} cm^{-1} (Hudson & Weber, 1973). This labeling procedure typically resulted in 0.6−0.7 molecule of AEDANS per Fab' molecule. Fab−AEDANS concentrations in the range of 0.5−2 μM were used in fluorescence measurements.

Isothermal Polarization Plots. Preliminary to performing time-resolved anisotropy studies, isothermal polarization (Perrin) plots were used to determine whether or not the Fab−AEDANS conjugate exhibited more than one rotational component. In such experiments, the viscosity of the solution was varied by addition of sucrose, and the fluorescence polarization (or anisotropy) of the labeled Fab was measured after each addition. Data were analyzed by plotting reciprocal anisotropy ($1/r$) versus the ratio of absolute temperature to viscosity (T/η). If the Fab acts as a rigid rotor, then a linear Perrin plot will be observed that can be fitted using the equation:

$$\frac{1}{r} = \frac{1}{r_0} + \left(\frac{R\tau}{r_0 V}\right)\frac{T}{\eta} \tag{1}$$

where r_0 is intrinsic (or limiting) anisotropy, τ is the fluorescence lifetime of the fluorescence label, R is the gas constant, and the slope of the plot is related to the hydrodynamic volume (V) of the molecule (Wahl & Weber, 1967). However, if segmental motion occurs within the Fab (*i.e.*, motion of the C_L-C_H1 domain dimer relative to the V_L-V_H domain dimer), then at least two different rotational rates will be observed (one for the global rotation of the Fab and a second for segmental motion within the Fab), which will result in nonlinear Perrin plots. Such plots can be analyzed using the following modification of the Perrin equation:

$$r = r_0\left[\frac{f_1}{1+\beta_1\left(\frac{T}{\eta}\right)} + \frac{1-f_1}{1+\beta_2\left(\frac{T}{\eta}\right)}\right] \tag{2}$$

$$\beta_1 = \frac{\tau}{\theta_1}\left(\frac{\eta}{T}\right)_{wat} \qquad \beta_2 = \frac{\tau}{\theta_2}\left(\frac{\eta}{T}\right)_{wat} \tag{3}$$

where θ_1 is the rotational correlation time associated with the global motion of the molecule, θ_2 the rotational correlation time associated with the local motion of the molecule

and/or fluorescent probe, f_1 the fraction of the limiting anisotropy which is associated with θ_1, and $(\eta/T)_{wat}$ the viscosity to temperature ratio for water at temperature T (Wahl & Weber, 1967).

Steady-state fluorescence anisotropy measurements of Fab−AEDANS were made at various sucrose concentrations using a spectrofluorometer (ISS, Model K2, Champaign, IL). Samples were excited with the 364 nm line of an argon ion laser (Spectra Physics, Model 2045, Mountain View, CA). Emission at wavelengths greater than 435 nm was viewed through a Schott GG 455 long-pass filter. Anisotropy measurements were taken at three different temperatures (10, 25, and 35 °C) for solutions of the Fab−AEDANS conjugate alone and for the conjugate saturated with fluoresceinamine (FLM) (Aldrich Chemicals, Milwaukee, WI). Fluoresceinamine had been previously purified by FPLC to remove residual fluorescein. The quantum yield of fluorescein is 200 times greater than that of FLM (Herron, 1984), so even a minute amount of fluorescein would give rise to a significant background signal.

A stock mixture of 66% w/w sucrose (Sigma Chemicals) solution was prepared. Water content in sucrose crystals was measured by vacuum drying the sucrose at 70 °C for 3 h. The weight difference in the sucrose before and after drying was less than 0.05%. Identical aliquots of sucrose were added to both of the Fab−AEDANS solutions (with and without FLM) and to a reference buffer solution (used for scatter correction). Viscosity values were obtained for each sucrose concentration by applying a fourth-order polynomial curve fit to viscosity versus sucrose concentration data, which was obtained from literature sources (Swindells *et al.*, 1958; Weast, 1981).

Phase-Modulation Fluorescence Lifetime and Anisotropy Measurements. The reader is referred to articles by Spencer and Weber (1969) and Jameson *et al.* (1984) for a complete description of phase-modulation fluorescence spectroscopy. Briefly, the exciting light is modulated at a specific frequency, and the phase shift and relative modulation of the fluorescence emission are measured with respect to the excitation source or a reference lifetime. Modulation frequencies in the range of 2−100 MHz were used to measure the fluorescence lifetime of AEDANS, which is typically in the range of 10−20 ns.

Phase and modulation measurements of the Fab−AEDANS conjugate were performed at the above three temperatures (10, 25, and 35 °C) using the ISS K2 spectrofluorometer. The Fab−AEDANS solution was titrated with FLM at each temperature. At 10 °C, mole ratios (FLM to Fab−AEDANS) of 0.0, 0.12, 0.24, 0.36, and 0.48 were used. At 25 °C, these ratios were 0.0, 0.12, 0.24, 0.48, and 0.96; and at 35 °C, they were 0.0, 0.24, 0.48, 0.96, and 1.44. The same preparation of Fab−AEDANS was used at all three temperatures. For each combination of temperature and mole ratio, two data sets were taken—one which consisted of phase and modulation lifetime determinations performed at 12 different modulation frequencies (logarithmically spaced between 2 and 100 MHz) and a second which consisted of phase and modulation anisotropy determinations at the same frequencies. The argon ion laser was tuned to the 364 nm line, and emission at wavelengths greater than 380 nm was viewed through a Schott GG 400 long-pass filter. For lifetime measurements, the exciting light was polarized vertically while emission was monitored through a polarizer oriented at 54.7° from the vertical to eliminate polarization effects (Spencer & Weber, 1969). For AEDANS lifetime measurements, POPOP [1,4-bis(5-phenyl-2-oxazolyl)benzene; 2,2′-*p*-phenylenebis(5-phenyloxazole), τ = 1.35 ns] (Kodak Chemicals, Rochester, NY) was used as a reference, while fluorescein (τ = 4.0 ns) (Molecular Probes) was used as a reference for FLM.

Analysis of Phase and Modulation Data. Phase and modulation lifetime data were analyzed using the nonlinear least squares procedure described by Jameson *et al.* (1984). In this method, phase and modulation values are calculated for a system of two or more noninteracting fluorescent species (or components) using the equations:

$$P_c = \tan^{-1}(S(\omega)/G(\omega)) \qquad M_c = \sqrt{S(\omega)^2 + G(\omega)^2} \tag{4}$$

$$S(\omega) = \sum_i \frac{f_i \omega \tau_i}{1 + (\omega\tau_i)^2} \qquad G(\omega) = \sum_i \frac{f_i}{1 + (\omega\tau_i)^2} \tag{5}$$

where P_c is the calculated phase value, M_c is the calculated modulation value, τ_i is the fluorescence lifetime of the ith component, f_i is its contribution to the total fluorescence intensity, and ω is the angular modulation frequency. Alternately, $S(\omega)$ and $G(\omega)$ can be determined from a distribution of lifetimes [$f(\tau)$] rather than a discrete sum, as described by Alcala *et al.* (1987a):

$$S(\omega) = \int \frac{f(\tau)\omega\tau}{1 + (\omega\tau)^2} d\tau \qquad G(\omega) = \int \frac{f(\tau)}{1 + (\omega\tau)^2} d\tau \tag{6}$$

Calculated phase and modulation values (P_c and M_c) are fit to measured phase (P_m) and modulation (M_m) values using the expression for reduced χ^2:

$$\chi^2 = \frac{\sum\left[\left(\frac{P_m - P_c}{\sigma_p}\right)^2 + \left(\frac{M_m + M_c}{\sigma_m}\right)^2\right]}{2n - f - 1} \tag{7}$$

where the sum is taken over P_m and M_m values measured at n different modulation frequencies, σ_p and σ_m are the standard errors of each phase and modulation measurement, respectively, and f is the number of free parameters. The reduced χ^2 value is minimized by varying τ_i and f_i in eq 5 or 6.

Phase and modulation anisotropy data were analyzed as described by Hazlett *et al.* (1989). In brief, the difference in phase angle ($\Delta\Phi$) between the parallel and perpendicular components of the fluorescence emission, as well as the ratio of their ac signals (Y), can be measured directly as a function of modulation frequency. In the case of isotropic rotation these parameters are related to the rotational diffusion constant (D) of the fluorophore (Weber, 1977):

$$\Delta\Phi = \tan^{-1}\left(\frac{3\omega r_0 6D}{(k^2 + \omega^2)(1 + r_0 - 2r_0^2) + 6D(6D + 2k + kr_0)}\right) \tag{8}$$

$$Y = \sqrt{\frac{[(1 - r_0)k + 6D]^2 + (1 - r_0)^2\omega^2}{[(1 + 2r_0)k + 6D]^2 + (1 + 2r_0)^2\omega^2}} \quad (9)$$

where r_0 is the limiting anisotropy and k is the radiative decay constant ($1/\tau$). For isotropic rotation, the rotational diffusion constant is inversely related to the rotational correlation time [$\theta = (1/6)D$]. Although several different approaches can be applied to analyzing heterogeneous anisotropy data (as obtained for the Fab−AEDANS conjugate), the most appropriate for Fab-AEDANS is a model that contains two rotational components—one (θ_1) that describes the unrestricted rotation of the entire Fab and a second (θ_2) that describes the restricted local (or segmental) motion of the AEDANS moiety attached to the constant domain dimer. In the time domain such a model can be described by eq 10, provided that $\theta_1 \gg \theta_2$ (Lipari & Szabo, 1980; Jameson & Hazlett, 1991):

$$r(t) = r_0(f_1 e^{-t/\theta_1} + f_2 e^{-t/\theta_2}) \quad (10)$$

where f_1 and f_2 are the fractional changes in fluorescence anisotropy associated with θ_1 and θ_2, respectively. Equation 10 was transformed into the frequency domain as described by Weber (1977).

Global Analysis. Data obtained from different experimental conditions (*e.g.*, different temperatures and FLM:Fab ratios) can be fitted simultaneously in a global analysis (Beechem *et al.*, 1985; Beechem & Gratton, 1988; Beechem, 1992). This technique is well suited to establish relations that may exist between different decay curves and suggest real physical models to describe the underlying experimental system (Beechem & Gratton, 1988). Phase-modulation lifetime and anisotropy data sets were subjected to global analysis using Rosenbrock's algorithm for a multivariable nonlinear function with constraints (Kuester & Mize, 1973). This algorithm is a sequential search technique without the use of derivatives. The algorithm evaluates the nonlinear function as both the direction of change and the step size are varied for each parameter without violating its constraint conditions. The global analysis program was written in FORTRAN and run on the Silicon Graphics Iris (SGI) 4D/220S computer. Standard errors of 0.4° for phase and 0.01 for modulation were used for the χ^2 minimization of both the lifetime and anisotropy data.

RESULTS

Labeling of Fab′ Fragments with AEDANS. After digestion of the antibody with pepsin and purification of F(ab′)$_2$ fragments, sodium dodecyl sulfate−polyacrylamide gel electrophoresis (SDS−PAGE) was used to evaluate sample purity (data not shown). Undigested antibody and Fab fragments were observed in the F(ab′)$_2$ fractions obtained from the Superdex column, but only F(ab′)$_2$ fragments were observed after the subsequent chromatofocusing step. The pH range of the F(ab′)$_2$ fractions from the latter separation was between 8.3 and 8.6. The final yield of F(ab′)$_2$ was low; starting with 30 mg of IgG, about 6 mg of the F(ab′)$_2$ was obtained.

The consensus hinge region sequence (216H-EPRGPIK-PCPPCKCP-230H, Kabat *et al.*, 1991) of a murine IgG$_{2a}$ heavy chain (such as found in 4−4−20) contains three cysteine residues. The 1 mM DTT concentration used in these studies effectively reduced these disulfide bonds; lower DTT concentrations resulted in incomplete cleavage of the F(ab′)$_2$ fragments. Because digestion of the antibody with pepsin results in F(ab′)$_2$ fragments with one or more of these disulfide bonds, after the reaction with DTT, there is a distribution of Fab′ fragments that differ in C-terminal length by a few residues. The purity of both the Fab′ fragment and the Fab−AEDANS conjugate was assessed using SDS−PAGE and nondenaturing polyacrylamide gel electrophoresis (ND-PAGE) (data not shown). Further, ND-PAGE indicated that there were three different species of the Fab−AEDANS conjugate. Because the degree of labeling was relatively low (0.6−0.7 AEDANS group per Fab′), any given Fab′ molecule probably contained only one fluorescent dye. Furthermore, it is unlikely that the heavy and light chains of the Fab′ could dissociate during the reaction with DTT and exist separately in solution because their preponderance for association is very high (Kranz & Voss, 1981b).

In addition to the results of gel electrophoresis, fluorescence measurements also support the above conclusions. A soluble AEDANS−cysteine conjugate was prepared in order to compare the spectral properties of the dye both in bulk solution and attached to the protein. The soluble conjugate exhibited an emission maximum of 500 nm, while a value of 488 nm was observed for the Fab−AEDANS conjugate. Furthermore, the fluorescence intensity (and quantum yield) of the soluble conjugate was only about one-quarter of that observed for the Fab-AEDANS conjugate. Taken together, these two results suggest that the microenvironment of AEDANS was significantly less polar when attached to the Fab′ than when free in solution. Furthermore, time-resolved measurements showed that the fluorescence lifetime of the soluble conjugate (*ca.* 10 ns) was invariant at three different temperatures (10, 25, and 35 °C), while that of Fab−AEDANS decreased from 16.8 to 15 ns over this temperature range (see section on lifetime measurements, below). Such a decrease is often indicative of environmental heterogeneity; *i.e.*, AEDANS, when attached to the Fab′, experiences more than one microenvironment. Finally, the antigen-binding affinity of the F(ab′)$_2$ and the Fab−AEDANS conjugate was measured using a fluorescence quenching assay (Herron, 1984). The affinity of the two preparations was essentially the same, which indicated that the conjugation reaction did not adversely affect the antigen-binding capacity of the antibody.

Analysis of Fluorescence Lifetimes of Labeled Fab′ Fragments. In order to determine rotational correlation times from fluorescence anisotropy data, it is necessary to know the fluorescence lifetime of the fluorescent probe. For this reason, phase and modulation measurements were taken at several different temperatures and FLM:Fab ratios for the Fab−AEDANS conjugate. Three different fluorescent species were considered in the lifetime analysis—AEDANS attached to the unliganded Fab, AEDANS attached to the Fab−FLM complex, and FLM itself. The lifetime and fluorescence intensity of FLM were much smaller than those of AEDANS, but the contribution of the former was significant at high frequencies and hence was included in the analysis. Initially, the lifetime data were fit using three discrete components; however, this model gave relatively high χ^2 values, so distributed lifetime models were investigated. As described above, there were several potential attachment sites for AEDANS in the C-terminus of the Fab′,

which could differ slightly from one another in their chemical environments and affect the fluorescent decay rate of the probe (Alcala *et al.*, 1987a,b). Thus, distributed lifetimes (using a Lorentzian distribution function) were used for both the unliganded and bound species of the Fab−AEDANS, while a discrete lifetime was employed for FLM.

Global analysis was used to fit simultaneously the phase and modulation data obtained at the three temperatures (Beechem *et al.*, 1985; Beechem & Gratton, 1988; Beechem, 1992). The following activation energy equation was used to link lifetime values as a function of temperature (Bushueva *et al.*, 1978; Rosato *et al.*, 1990):

$$\tau = [K_1 + K_0 \exp(-E/RT)]^{-1} \quad (11)$$

where τ is the lifetime, K_1 the radiative decay rate, K_0 the nonradiative thermal rate constant at infinite temperature, and E the activation energy for thermal quenching. This expression is consistent with traditional views about the depopulation of the excited state; fluorescence emission occurs at rate K_1, while the rate of nonradiative processes is described by a Boltzman distribution [$K_0 \exp(-E/RT)$].

Because of the number of data sets involved, a preliminary global analysis was performed using only those data sets without FLM in order to estimate the fluorescence lifetime of the unliganded Fab−AEDANS conjugate. A second preliminary analysis was performed using only data sets with a mole ratio of 0.96 in order to obtain estimates for the other two fluorescent species (liganded Fab−AEDANS conjugate and FLM). Next, a three-component analysis was performed separately at each temperature to optimize lifetime fraction parameters (the lifetimes and distributions were held fixed during this optimization). Then all the data sets were combined, and the activation energy parameters and distributions were optimized with the fractions held fixed. Finally, all parameters were allowed to vary.

Results of the final lifetime analysis are shown in Table 1 and Figure 1. As mentioned above, the lifetime of the Fab−AEDANS conjugate decreased from 16.8 ns at 10 °C to 15.0 ns at 35 °C. These values decreased by an additional 14% upon binding of FLM. Global analysis suggested that this latter decrease was due to an increase in the radiative decay rate K_1 from 0.006 to 0.015 ns^{-1} (Table 1), a result which was consistent with an energy transfer mechanism (excited-state energy was transferred from AEDANS to FLM, which decreased the fluorescence lifetime of the former). The width of the lifetime distribution also decreased when FLM was bound to the Fab. In addition, the fractional contribution of each lifetime varied in proportion to the amount of FLM added. The higher K_1 rate observed for FLM than that observed for either of the AEDANS−Fab species resulted in a shorter lifetime. Finally, analysis of phase-modulation data obtained for the AEDANS−cysteine sample (data not shown) showed no significant difference in χ^2 between discrete and distributed lifetime models. In both cases, the lifetime was 10 ns for AEDANS−cysteine, and the lifetime width from the Lorentzian distribution analysis was 0.3 ns.

Steady-State Anisotropy Measurements. As mentioned in the introduction, the segmental flexibility of immunoglobulins has previously been investigated at the level of Fab and Fc fragments, but few if any studies have examined segmental motions within these fragments. Thus, isothermal polarization (Perrin) plots were used to determine whether

Table 1: Results of Global Analysis of Phase-Modulation Lifetime Data

(A) Linking Activation Energy Parameters[a]

	Fab−AEDANS	Fab−AEDANS + FLM	FLM
K_1 (ns^{-1})	0.006 (0.001−0.022)	0.015 (0.007−0.028)	1.997 (1.500−4.900)
K_0 (ns^{-1})	0.254 (0.210−0.300)	0.268 (0.230−0.320)	0.263 (0.001−3.480)
E (kcal/mol)	0.874 (0.730−0.970)	0.899 (0.740−1.010)	0.023 (0.001−5.500)

(B) Lifetimes (τ) and Lorentzian Distribution Widths (σ) for AEDANS and FLM[b]

	Fab−AEDANS		Fab-AEDANS + FLM		FLM
temp (°C)	τ (ns)	σ (ns)	τ (ns)	σ (ns)	τ (ns)
10	16.80	3.67	14.37	3.03	0.44
25	15.65	3.37	13.49	2.65	0.44
35	14.97	3.39	12.97	2.40	0.44

(C) Lifetime Fractions and χ^2 Values for Phase-Modulation Data Sets[c]

		lifetime fractions			
temp (°C)	FLM:Fab ratio	f_1	f_2	f_3	individual χ^2
10	0.00	0.989	0.008	0.003	1.79
	0.12	0.880	0.102	0.018	0.73
	0.24	0.735	0.232	0.033	0.82
	0.36	0.653	0.296	0.051	1.01
	0.48	0.539	0.393	0.068	0.75
25	0.00	0.988	0.008	0.004	0.58
	0.12	0.887	0.102	0.011	0.74
	0.24	0.748	0.228	0.024	1.00
	0.48	0.504	0.450	0.046	0.92
	0.96	0.051	0.859	0.090	1.08
35	0.00	0.990	0.008	0.002	1.24
	0.24	0.758	0.227	0.015	1.22
	0.48	0.508	0.456	0.036	1.60
	0.96	0.055	0.864	0.081	0.80
	1.44	0.010	0.900	0.090	0.77

[a] Average values and 95% confidence limits (shown in parentheses) were listed for linking parameters that were defined in eq 11. These values were determined from a global fit of 15 phase-modulation lifetime data sets obtained at different temperatures and FLM:Fab ratios. Three lifetime components were extracted from the global analysis—one for the unliganded Fab-AEDANS conjugate (Fab−AEDANS), a second for Fab−AEDANS saturated with FLM (Fab−AEDANS + FLM), and a third for FLM bound to the Fab. In the error analysis, each parameter was held fixed while other parameters were varied to minimize χ^2 (Beechem, 1992). The F-statistic was used to determine 95% confidence intervals. [b] Fluorescence lifetime values were computed from the above linking parameters. Distributed lifetimes were used for Fab−AEDANS and Fab−AEDANS + FLM, while a discrete lifetime was used for FLM. [c] Lifetime fractions (f_1, Fab−AEDANS; f_2, Fab−AEDANS + FLM; f_3, FLM) and individual χ^2 values are shown for each data set. A global χ^2 value of 0.89 was obtained for the fit of all data sets.

or not such motions could be observed in the 4−4−20 Fab. Such plots are well suited for this purpose because they are much easier to perform than dynamic anisotropy measurements and can differentiate between global and segmental rotations.

Isothermal Perrin plots are shown in Figure 2 for Fab−AEDANS, with and without FLM, at three different temperatures (10, 25, and 35 °C). The limiting anisotropy values (*i.e.*, y-intercept values) for these plots were determined by measuring the anisotropy of Fab−AEDANS in sucrose solution at −10 °C with 364 nm excitation. This procedure gave r_0 values of 0.32 and 0.30 for Fab−AEDANS without and with FLM, respectively. (FLM itself gave a near-zero anisotropy from a very low fluorescence signal with 364 nm

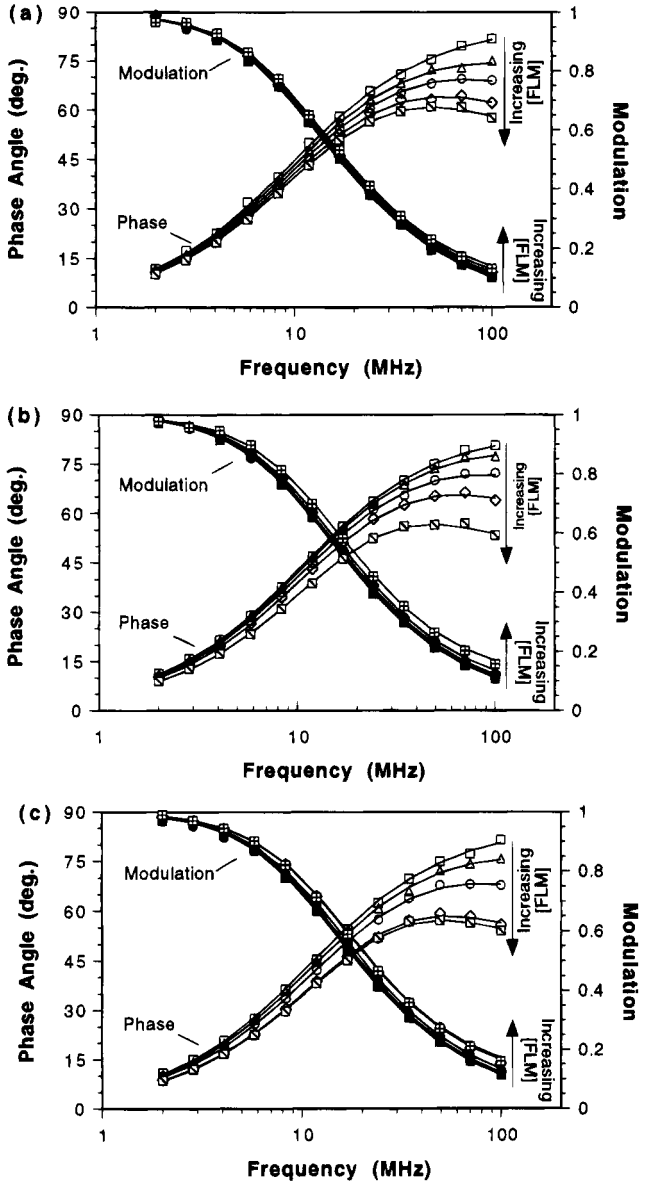

FIGURE 1: Phase-modulation fluorescence lifetime data for the titration of Fab−AEDANS with FLM at (a) 10 °C, (b) 25 °C, and (c) 35 °C. The Fab−AEDANS conjugate was titrated at each temperature with four different concentrations of fluoresceinamine (FLM), which resulted in the following FLM:Fab mole ratios: 10 °C (panel a) 0.0, 0.12, 0.24, 0.36, 0.48; 25 °C (panel b) 0.0, 0.12, 0.24, 0.48, 0.96; and 35 °C (panel c) 0.0, 0.24, 0.48, 0.96, 1.44. Plot symbols: experimentally determined phase-modulation lifetime data. Solid lines: global fits based on the three-component lifetime model described in the text.

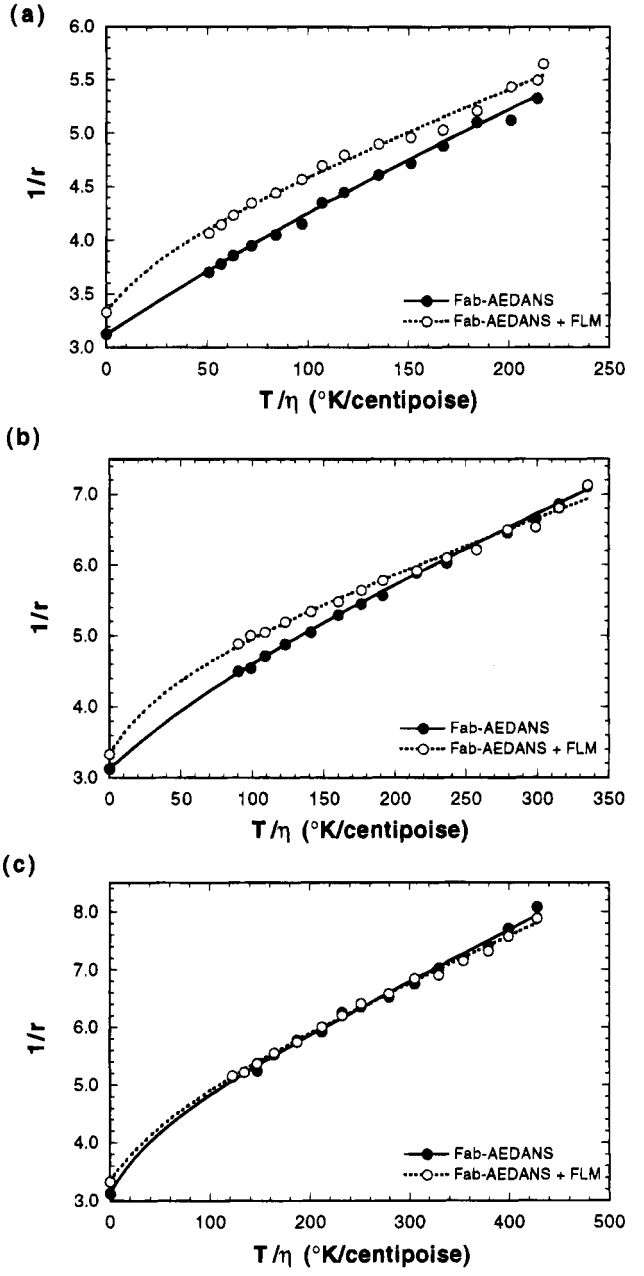

FIGURE 2: Steady-state anisotropy measurements for the unliganded and liganded 4−4−20 Fab−AEDANS conjugate at (a) 10 °C, (b) 25 °C, and (c) 35 °C. Symbols: closed circles, unliganded Fab−AEDANS conjugate; open circles, Fab−AEDANS with fluoresceinamine (FLM). Solid and dashed lines: nonlinear least squares fits based on eq 2 and 3.

excitation at −10 °C in 1:2 glycerol solution.) Curvilinear plots were observed in all cases, which indicated the presence of at least two rotational components. Further, at two temperatures (10 and 25 °C) plots were well differentiated for Fab−AEDANS with and without FLM, which suggested that the hydrodynamic behavior of these two species may be different. All six plots were fit using eq 2 and 3, but correlation times determined by this method were relatively imprecise. For example, values of 27 ± 12 and 4.0 ± 2.1 ns (mean ± standard error) were determined for θ_1 and θ_2 of Fab−AEDANS without FLM, respectively. Comparable (or larger) errors were observed for the five other fittings. This imprecision was probably due to the lack of data points at T/η values near zero (an experimental limitation), a region that contains information about the local motion of the macromolecule. As a consequence, there was not enough resolving power in the experimental data to make a clear separation between the two correlation times for each of the Fab−AEDANS species. Thus, isothermal Perrin plots alone were probably not sufficient to demonstrate the differences in the Fab before and after binding of the antigen.

Dynamic Anisotropy Measurements. Phase-modulation anisotropy measurements are better equipped than isothermal Perrin plots to resolve subtle differences in rotational components for several reasons. First, rotational correlation times in the range of 0.1 ns to several hundred nanoseconds can be determined accurately using modern phase-modulation instrumentation without varying solution viscosity (Jameson *et al.*, 1984; VanderMeulen *et al.*, 1990; Brunet *et al.*, 1993). Second, two or more rotational correlation times can be

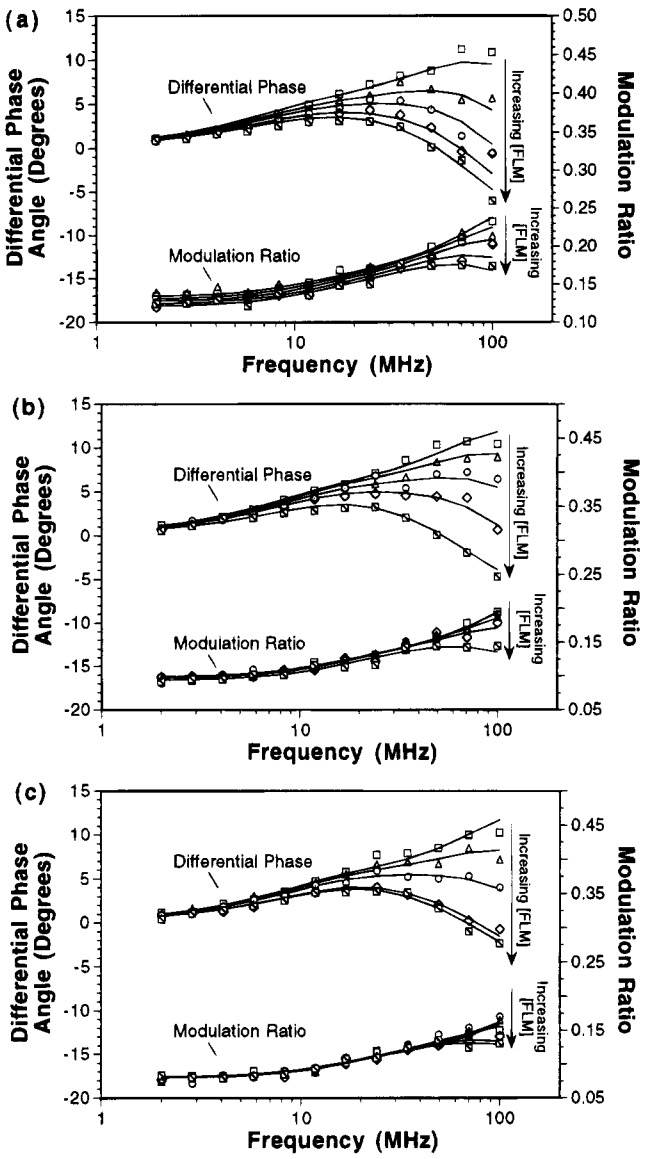

FIGURE 3: Phase-modulation anisotropy data for the titration of Fab−AEDANS with FLM at (a) 10 °C, (b) 25 °C, and (c) 35 °C. The Fab−AEDANS conjugate was titrated at each temperature with four different concentrations of fluoresceinamine (FLM), which resulted in the following FLM:Fab mole ratios: 10 °C (panel a) 0.0, 0.12, 0.24, 0.36, 0.48; 25 °C (panel b) 0.0, 0.12, 0.24, 0.48, 0.96; and 35 °C (panel c) 0.0, 0.24, 0.48, 0.96, 1.44. Plot symbols: experimentally determined phase-modulation lifetime data. Solid lines: global fits based on the three-component lifetime model described in the text.

resolved by taking a series of measurements over a wide (1−100 MHz, or higher) frequency range (VanderMeulen *et al.*, 1990; Brunet *et al.*, 1993). Third, global analysis enables data sets obtained under different conditions to be analyzed for common factors or parameters (Beechem *et al.*, 1985; Beechem & Gratton, 1988; Beechem, 1992).

Given that the Fab−AEDANS conjugate was titrated with FLM, global analysis was performed for a two-rotational component model that contained the three lifetime components described above (Figure 3). Although each lifetime was associated with two different rotational correlation times, only four rotational correlation times were optimized in the analysis because two of the lifetimes (AEDANS attached to the unliganded Fab and FLM bound to Fab−AEDANS) were both associated with the same motions of the liganded Fab. FLM was included in the analysis because its effects—though very small due to a near-zero r_0 value at 364 nm excitation—were important at high frequencies.

As with the lifetime data, a temperature-dependent equation was used to link the anisotropy data in global analysis. If the slower correlation time (θ_1) was correlated to the global motion of the Fab, the Stokes−Einstein relation could be used to describe the temperature dependency:

$$\theta_1 = \frac{V\eta}{RT} = \frac{4\pi R_s^3 \eta}{3RT} \tag{12}$$

where V is the hydrated molecular volume of the rotating species and R_s is the radius of an equivalent sphere. This equation was used to link θ_1 across the three temperatures using R_s as a common parameter to be fitted.

The faster correlation time (θ_2) might also be related to its own diffusion coefficient. However, the presence of two parameters related to diffusion coefficients in the same global analysis caused the curve-fitting routine to equalize these two parameters. An alternative linking strategy was based on the assumption that θ_2 was correlated to segmental motion of the Fab and/or motion of the fluorescent probe. Since the fluorescence emission properties of Fab−AEDANS suggested that the probe was buried in a relatively nonpolar region, it seemed reasonable to assume that any motion of the probe would require overcoming an activation energy barrier (E):

$$\theta_2 = [A \exp(-E/RT)]^{-1} \tag{13}$$

where A is a preexponential constant. In contrast to the rotational correlation times, the fractional contributions to the limiting anisotropy (f_1 and f_2; $f_2 = 1 - f_1$) seemed to exhibit a more complex relation as a function of temperature (Weber, 1989). Their linkage across different temperatures was not successful, and hence they were allowed to vary independently of temperature.

Three sets of global analyses were performed—one in which all data sets were fitted simultaneously using the above linking strategies, a second in which separate analyses were performed for the unliganded Fab (FLM:Fab ratio of 0.0) and the Fab saturated with FLM (FLM:Fab ratio of 0.96), and a third in which data sets obtained at each temperature were fitted separately. The purpose in performing the latter two sets of analyses was mostly confirmatory, *i.e.*, to show that the linking strategies did not unduly bias the results. Global analyses were started with the same sets of initial parameter values for both species of the Fab−AEDANS conjugate. The experimentally derived values of limiting anisotropy r_0 of each of the two forms of the conjugate were used as fixed parameters. The optimum value of preexponential constant A was determined by performing a preliminary series of minimizations in which A was varied until the minimum χ^2 value was found, and then it was fixed in subsequent minimizations. The old parameters were replaced with newly fitted values until no further improvements in the global χ^2 were achieved.

Average values and 95% confidence limits are shown in Table 2 for the linking parameters defined in eq 12 and 13 for the global analysis which included all data sets. Two sets of linking parameters were determined—one for the unliganded Fab (Fab−AEDANS) and a second for the liganded Fab, saturated with FLM (Fab−AEDANS + FLM).

Table 2: Results of Global Analysis of Phase-Modulation Anisotropy Data Including All Data Sets

(A) Linking Parameters[a,b]

	Fab−AEDANS	Fab−AEDANS + FLM	FLM
limiting anisotropy r_0	0.32	0.30	−0.016 (−0.029 to +0.001)
radius of equivalent sphere (Å)	33.1 (31.1−35.5)	31.1 (27.7−35.4)	
preexponential constant A (ns^{-1})	1700	1700	
activation energy E (kcal/mol)	4.46 (4.40−4.52)	4.71 (4.55−4.84)	

(B) χ^2 Values for Individual Data Sets[c]

FLM:Fab ratio	temp (°C) 10	25	35
0.00	1.51	1.68	2.06
0.12	2.27	0.68	nd
0.24	1.72	1.96	1.61
0.36	3.13	nd	nd
0.48	1.22	1.13	1.27
0.96	nd[d]	1.00	0.75
1.44	nd	nd	0.85

[a] Average values and 95% confidence limits (shown in parentheses) are listed for linking parameters that were defined in eq 12 and 13. These values were determined from a global fit of 15 phase-modulation anisotropy data sets obtained at different temperatures and FLM:Fab ratios. Linking parameters were then used to calculate average values (and 95% confidence limits) for the rotational correlation times and anisotropy fractions listed in Table 3A. In the error analysis, each parameter was held fixed while other parameters were varied to minimize χ^2 (Beechem, 1992). The F-statistic was used to determine 95% confidence intervals. [b] Limiting anisotropy (r_0) values for Fab−AEDANS and Fab−AEDANS + FLM were determined experimentally and fixed in the global analysis, while the r_0 value of FLM was allowed to vary. Values of the preexponential constants (A) were determined as described in the text and then fixed in the global analysis. [c] A global χ^2 value of 1.31 was obtained for the fit of all data sets. [d] nd: not determined. Phase-modulation anisotropy measurements were made for samples with five different FLM:Fab ratios at each temperature. However, a slightly different set of five ratios was examined in each case. This was because the affinity of the 4−4−20 Fab decreases with increasing temperature (Gibson *et al.*, 1988) and a wider range of FLM:Fab ratios was required at the higher temperatures to ensure that the Fab would be fully saturated with FLM.

Although overlapping confidence limits were observed for the radius of an equivalent sphere (R_s) for the unliganded and liganded species of the Fab, nonoverlapping confidence intervals were observed for the activation energy (E) associated with segmental or local motion. The linking parameters were then used to derive rotational correlation times (θ_1 and θ_2) and anisotropy fractions (f_1 and f_2) for the unliganded and liganded species of the Fab at all three temperatures. These values (along with 95% confidence limits) are shown in Table 3A. As with the linking parameters, overlapping confidence limits were observed for the rotational correlation time (θ_1) associated with global motion for the unliganded and liganded species of the Fab, while nonoverlapping confidence intervals were observed for the correlation time (θ_2) associated with local or segmental motion. Interestingly, overlapping confidence limits were also observed for f_1, the anisotropy fraction associated with θ_1 (confidence limits were not determined for f_2 because its value is completely determined by f_1). Taken together, the above findings suggest that antigen binding produces a significant increase in the local or segmental motion of the constant domain dimer. This change, however, has little if any effect on the global rotation of the Fab.

As mentioned above, two additional sets of global analyses were performed to confirm the above results. In the first of these, separate fittings were performed for the Fab with FLM: Fab ratios of 0.0 and 0.96. These FLM:Fab ratios were at opposite ends of the active site saturation scale and thus were equivalent to the unliganded Fab and the Fab saturated with FLM, respectively. Rotational parameters (θ_1, θ_2, and f_1) determined by these fittings were comparable to those obtained from the global fit including all data sets (compare parts A and B of Table 3). In the second set of confirmatory analyses, separate global fits were performed at each temperature. Linking parameters (eq 12 and 13) were not used in these analyses because all data sets within one fit were obtained at the same temperature. The results of these analyses were again comparable to those obtained to the global analysis including all data sets (compare parts A and C of Table 3), which indicated that employment of linking parameters did not unduly bias the fitting process.

DISCUSSION

Labeling of Fab′ Fragments with AEDANS. The procedure of labeling the Fab′ with 1,5-IAEDANS involves preparation of $F(ab')_2$ fragments and cleavage of disulfide bonds with DTT to form Fab′ fragments. Although the dye may react with other functional groups such as amines, it prefers sulfhydryl groups. After the $F(ab')_2$ is treated with DTT, the most probable conjugation sites are the reduced disulfide bonds at the C-terminus of the Fab. The Fab−AEDANS conjugate exhibited both a higher fluorescence intensity and a shorter emission maximum than a soluble AEDANS−cysteine conjugate, which indicated that the label was attached to the Fab in a hydrophobic environment. Moreover, the lifetime of the dye in the Fab−AEDANS conjugate decreased with increasing temperature, which is usually indicative of a heterogeneous microenvironment. In contrast, the lifetime of soluble AEDANS−cysteine was independent of temperature. Taken together, these observations suggest strongly that AEDANS effectively became part of the Fab.

Fluorescence Lifetime Measurements. Phase-modulation lifetime data were fitted with distributed lifetimes because the multiple sulfhydryl sites available to the AEDANS label produced a heterogeneous chemical environment. Distributed lifetimes were applied to the two forms of AEDANS but not to FLM. The distribution of lifetimes for bound FLM should be very narrow or almost discrete. In addition, the lifetime of FLM and its contribution to the observed fluorescence intensity were very small compared to those of AEDANS with 364 nm excitation. For AEDANS attached to the Fab in either the presence or absence of FLM, the width of the lifetime distribution decreased only by 0.4 ns from 10 to 25 °C and showed almost no change when the temperature was increased to 35 °C. This result indicated that AEDANS experienced some local motion even at 10 °C, but increased thermal fluctuations at higher temperatures did not significantly alter the chemical environment experienced by the dye. However, the difference in the widths of the distribution was consistently about 0.8 ns smaller for AEDANS attached to the liganded Fab at all three temperatures. This observation may be due to a conformational change that restricted the motion of AEDANS.

Table 3: Rotational Correlation Times and Corresponding Fractions from Global Analysis of Phase-Modulation Anisotropy Data[a]

	(A) Results from a Fitting of All Data Sets[b]							
	Fab−AEDANS				Fab−AEDANS + FLM			
temp (°C)	θ_1 (ns)	f_1	θ_2 (ns)	f_2	θ_1 (ns)	f_1	θ_2 (ns)	f_2
10	50.6 (42.1−62.7)	0.49 (0.45−0.52)	1.7 (1.5−1.8)	0.51	42.3 (29.8−62.2)	0.46 (0.36−0.60)	2.6 (1.9−3.1)	0.54
25	32.8 (27.3−41.0)	0.39 (0.36−0.43)	1.1 (1.0−1.2)	0.61	27.4 (19.3−40.2)	0.44 (0.37−0.51)	1.7 (1.3−2.0)	0.56
35	25.6 (21.3−31.7)	0.35 (0.31−0.38)	0.9 (0.8−1.0)	0.65	21.4 (15.1−31.4)	0.39 (0.33−0.46)	1.3 (1.0−1.6)	0.61
	(B) Results from Separate Fittings for Fab−AEDANS and Fab−AEDANS + FLM[c]							
	Fab−AEDANS				Fab−AEDANS + FLM			
temp (°C)	θ_1 (ns)	f_1	θ_2 (ns)	f_2	θ_1 (ns)	f_1	θ_2 (ns)	f_2
10	47.2 (39.4−57.5)	0.49 (0.45−0.52)	1.6 (1.5−1.8)	0.51	nd[d]	nd	nd	nd
25	30.6 (25.5−37.2)	0.41 (0.37−0.44)	1.1 (1.0−1.2)	0.59	28.8 (23.0−37.5)	0.45 (0.40−0.51)	1.8 (1.5−2.1)	0.55
35	23.9 (19.9−29.1)	0.36 (0.32−0.39)	0.9 (0.8−1.0)	0.64	22.5 (18.0−29.4)	0.39 (0.34−0.45)	1.4 (1.1−1.6)	0.61
	(C) Results from Separate Fittings of Each Temperature Data Set[e]							
	Fab−AEDANS				Fab−AEDANS + FLM			
temp (°C)	θ_1 (nsec)	f_1	θ_2 (ns)	f_2	θ_1 (ns)	f_1	θ_2 (ns)	f_2
10	61.3 (33.5−77.5)	0.47 (0.43−0.50)	1.7 (1.6−2.0)	0.53	60.0 (30.1−72.1)	0.41 (0.25−0.63)	3.3 (2.3−4.6)	0.59
25	33.6 (26.5−42.3)	0.39 (0.36−0.42)	1.2 (1.0−1.3)	0.61	28.2 (21.2−49.7)	0.43 (0.32−0.51)	1.7 (1.3−2.2)	0.57
35	19.8 (15.7−25.0)	0.37 (0.34−0.41)	0.8 (0.7−0.8)	0.63	20.6 (15.1−27.4)	0.39 (0.33−0.47)	1.3 (0.9−1.7)	0.61

[a] Average values and 95% confidence limits (shown in parentheses) are listed for each parameter. In the error analysis, each parameter was held fixed while other parameters were varied to minimize χ^2 (Beechem, 1992). The *F*-statistic was used to determine 95% confidence intervals. [b] Results of global analysis using all data sets. Data sets were linked across temperature using eq 12 and 13. Linking parameters and χ^2 values are given in Table 2. [c] Results of separate global analyses performed for Fab−AEDANS (left column) and for Fab−AEDANS + FLM (right column). In the former, data sets obtained at 10, 25, and 35 °C with an FLM:Fab ratio of 0.0 were linked across temperature using eq 12 and 13 (linking parameters not shown). A similar procedure was followed for Fab-AEDANS + FLM, except that data sets obtained at 25 and 35 °C with an FLM:Fab ratio of 0.96 were used instead. A global χ^2 value of 1.50 was obtained for Fab−AEDANS without FLM and a value of 0.76 for Fab−AEDANS with FLM. [d] nd: not determined. Rotational correlation times were not determined at 10 °C in this analysis because phase and modulation measurements were not made at 10 °C for the Fab−AEDANS sample with an FLM:Fab ratio of 0.96. [e] Results of separate global analyses performed at each temperature as described in the text. In this case, the rotational correlation times and anisotropy fractions were the actual fitted parameters. Global χ^2 values of 1.10, 1.10, and 0.90 were obtained for data sets measured at 10, 25, and 35 °C, respectively.

Examination of the 95% confidence intervals for the activation energy parameters (Table 1) revealed a high degree of overlap for the nonradiative parameters (K_0 and E) between the unliganded and liganded forms of the Fab−AEDANS conjugate and a more modest overlap for the radiative rate K_1. Further, the lifetime distributions of the two forms of Fab−AEDANS overlapped to some degree as well. Taken together, these observations suggest that the microenvironment of the AEDANS probe is very similar in the two forms of the Fab−AEDANS conjugate. The difference in radiative rate, however, is probably due to fluorescence energy transfer as mentioned previously. Considering the global and individual χ^2 values for the data sets, we believe that our model reflects the chemical and physical state of the Fab−AEDANS samples examined. Furthermore, the activation energy parameters appear to be a suitable model to explain the behavior of the AEDANS probe at different temperatures.

Interestingly, the analysis could be performed to give lower χ^2 values if fewer restraints were applied. However, these analyses led to results which were nonsensical from a chemical perspective. For example, an analysis using discrete lifetime components showed a good fit but yielded AEDANS lifetime values of 18 and 9 ns for the unliganded and liganded species; more importantly, the lifetime fractions did not correspond to the amounts of FLM added—a clear chemical impossibility. Fitting the data separately for each temperature also gave unpredictable results.

Fluorescence Anisotropy Measurements. As with lifetimes, different models may be used to analyze dynamic anisotropy data. Because the Fab is approximately ellipsoidal in shape, anisotropy could be explained in terms of rotations about the principal axes of the ellipsoid (Brand *et al.*, 1985). This interpretation, however, is applicable only when the fluorophore is rigidly attached to the macromolecule. The fact that fractional contributions to the limiting anisotropy (f_1 and f_2) could not be made constant at different temperatures indicated a restricted flexibility of the label in relation to the macromolecule (Weber, 1989). The present anisotropy data were best fit with two rotational components. Whereas the larger rotational correlation time could be readily attributed to the global tumbling of the Fab, the second rotational correlation time could be a combination of both the local flexibility of the AEDANS label in the Fab and the segmental flexibility of the constant domain dimer (C_L−C_H1) to which it was attached.

The rotational correlation time of AEDANS free in solution is less than 0.4 ns [data not shown and Bucci *et al.* (1979)]. Furthermore, an estimate of the rotational correlation time of a freely rotating AEDANS group attached to a protein can be extrapolated from anisotropy studies of tryptophan residues in other proteins (an AEDANS group attached to the Fab is essentially another residue in the protein and therefore is analogous to the indole side chain of tryptophan). Depending on the chemical environment of tryptophan, its rotational correlation time can range from several picoseconds to a few nanoseconds (Lakowicz *et al.*, 1983; Chen *et al.*, 1988). Thus, if AEDANS were able to rotate freely, its rotational correlation time would be less than 1 ns even at 10 °C. On the basis of these observations, we believe that the second rotational correlation time of 2.6 ns (for the Fab−AEDANS conjugate with bound FLM at 10 °C) is most probably due to the restricted segmental motion of the Fab.

As mentioned in Results, θ_2 values determined for the unliganded and liganded species of the Fab were statistically different at all three temperatures (Table 3). Similar results were also obtained for the activation energy E associated with θ_2 (Table 2). These observations are consistent with our view that the structure of the Fab becomes more rigid when it binds the antigen—a prediction based on molecular dynamics simulations of the 4−4−20 Fab presented in the preceding paper (Lim & Herron, 1995). The extrapolated correlation times from these simulations exhibited differences between the Fab with and without fluorescein. Specifically, the simulations predicted that the rotational correlation time of a fluorescence probe attached to the C_L-C_H1 dimer should increase from 1.9 to 4.9 ns upon antigen binding. Although the predicted values are not very accurate due to the relatively short duration (174 ps) of the MD simulations, they are nevertheless consistent with the above observation that the liganded form of the Fab exhibits less local motion.

CONCLUSIONS

The main conclusion of these studies was that two rotational components were observed for the 4−4−20 Fab by both steady-state and dynamic anisotropy measurements—a longer correlation time that corresponded to the global rotation of the Fab and a shorter correlation time that was probably due to local and/or segmental motion of the constant domain (C_L-C_H1) dimer. Furthermore, dynamic anisotropy measurements indicated that the magnitude of the shorter correlation time increased by more than 50% upon antigen binding, suggesting that the conformation of the Fab may be more rigid in the liganded form.

The fitting of dynamic anisotropy data is often complicated by the complex nature of the molecular motions involved. Many types of models could have been employed to fit the observed phase and modulation values, as when separate analyses were performed for data collected at different temperatures. However, we have demonstrated that a unified approach, which consists of global analysis of both lifetime and dynamic anisotropy data coupled with chemical intuition, was able to resolve subtle differences in the dynamics of the 4−4−20 Fab induced by antigen binding. These observations could further be strengthened through additional fluorescence experiments, such as the use of different fluorescent labels or different excitation/emission wavelengths (Beechem *et al.*, 1985, 1986; VanderMeulen *et al.*, 1990; Brunet *et al.*, 1993). Finally, examination of macromolecular structure from a different perspective altogether is often invaluable. An example of this is the use of molecular dynamics simulations to examine in detail the conformational perturbations which occurred within the 4−4−20 Fab upon antigen binding (Lim & Herron, 1995).

REFERENCES

Alcala, J. R., Gratton, E., & Prendergast, F. G. (1987a) *Biophys. J. 51*, 587−596.

Alcala, J. R., Gratton, E., & Prendergast, F. G. (1987b) *Biophys. J. 51*, 597−604.

Beechem, J. M. (1992) *Methods Enzymol. 210*, 37−54.

Beechem, J. M., & Gratton, E. (1988) *Proc. SPIE-Int. Soc. Opt. Eng. 909*, 70−81.

Beechem, J. M., Ameloot, M., & Brand, L. (1985) *Anal. Instrum. 14*, 379−402.

Beechem, J. M., Knutson, J. R., & Brand, L. (1986) *Biochem. Soc. Trans. 14*, 832−835.

Brand, L., Knutson, J. R., Davenport, L., Beechem, J. M., Dale, R. E., Walbridge, D. G., & Kowalczyk, A. A. (1985) in *Spectroscopy and the Dynamics of Molecular Biological Systems* (Bayley, P. M., & Dale, R. E., Eds.) pp 259−305, Academic Press, New York.

Brunet, J. E., Vargas, V., Gratton, E., & Jameson, D. M. (1993) *Biophys. J. 66*, 446−453.

Bucci, E., Fronticelli, C., Flanigan, K., Perlman, J., & Steiner, R. F. (1979) *Biopolymers 18*, 1261−1276.

Bushueva, T. L., Busel, E. P., & Burstein, E. A. (1978) *Biochim. Biophys. Acta 534*, 141−152.

Cathou, R. E. (1978) in *Immunoglobulins* (Litman, G. W., & Good, R. A., Eds.) pp 37−83, Plenum Publishing, New York.

Chen, L. X.-Q., Engh, R. A., & Fleming, G. R. (1988) *J. Phys. Chem. 92*, 4811−4816.

Gibson, A. L., Herron, J. N., He, X.-M., Patrick, V. A., Mason, M. L., Lin, J.-N., Kranz, D. M., Voss, E. W., Jr., & Edmundson, A. B. (1988) *Proteins 3*, 155−160.

Hanson, D. C., Yguerabide, J., & Schumaker, V. N. (1981) *Biochemistry 20*, 6842−6852.

Hanson, D. C., Yguerabide, J., & Schumaker, V. N. (1985) *Mol. Immunol. 22*, 237−244.

Hazlett, T. L., Johnson, A. E., & Jameson, D. M. (1989) *Biochemistry 28*, 4109−4117.

Herron, J. N. (1984) in *Fluorescein Hapten: An Immunological Probe* (Voss, E. W., Jr., Ed.) pp 49−76, CRC Press, Boca Raton, FL.

Herron, J. N., Gentry, C. A., Davies, S. S., Wei, A.-P., & Lin, J.-N. (1994) *J. Controlled Release 28*, 155−166.

Hudson, E. N., & Weber, G. (1973) *Biochemistry 12*, 4154−4161.

Jameson, D. M., & Hazlett, T. L. (1991) in *Biophysical and Biochemical Aspects of Fluorescence Spectroscopy* (Dewey, T. G., Ed.) pp 105−133, Plenum Publishing, New York.

Jameson, D. M., Gratton, E., & Hall, R. D. (1984) *Appl. Spectrosc. Rev. 20*, 55−106.

Kabat, E. A., Wu, T. T., Perry, H. M., Gottesman, K. S., & Foeller, C. (1991) *Sequences of Proteins of Immunological Interest,* 5th ed., Vol. 1, National Institutes of Health, Bethesda, MD.

Kranz, D. M., & Voss, E. W., Jr. (1981a) *Mol. Immunol. 18*, 889−898.

Kranz, D. M., & Voss, E. W., Jr. (1981b) *Proc. Natl. Acad. Sci. U.S.A. 78*, 5807−5811.

Kuester, J. L., & Mize, J. H. (1973) *Optimization Techniques with FORTRAN*, McGraw-Hill Book Co., New York.

Lakowicz, J. R., Maliwal, B. P., Cherek, H., & Balter, A. (1983) *Biochemistry 22*, 1741−1752.

Lim, K., & Herron, J. N. (1995) *Biochemistry 34*, 6962−6974.

Lipari, G., & Szabo, A. (1980) *Biophys. J. 30*, 489−506.

Nezlin, R. (1990) *Adv. Immunol. 48*, 1−40.

Oi, V. T., Vuong, T. M., Hardy, R., Reidler, J., Dangle, J., Herzenberg, L. A., & Stryer, L. (1983) *Nature 307*, 136−140.

Parham, P. (1983) *J. Immunol. 131*, 2895−2902.

Pilz, I., Kratky, O., Licht, A., & Sela, M. (1973) *Biochemistry 12*, 4998−5005.

Pilz, I., Kratky, O., Licht, A., & Sela, M. (1975) *Biochemistry 14*, 1326−1333.

Rosato, N., Gratton, E., Mei, G., & Finazzi-Agrò, A. (1990) *Biophys. J. 58*, 817−822.

Sosnick, T. R., Benjamin, D. C., Novotny, J., Seeger, P. A., & Trewhella, J. (1992) *Biochemistry 31*, 1779−1786.

Spencer, R. D., & Weber, G. (1969) *Ann. N.Y. Acad. Sci. 158*, 361−376.

Swindells, J. F., Snyder, C. F., Hardy, R. C., & Golden, P. E. (1958) *Nat. Bur. Stand. Circ. (U.S.), Suppl. 440*, 1−7.

VanderMeulen, D. L., Nealon, D. G., Gratton, E., & Jameson, D. M. (1990) *Biophys. Chem. 36*, 177−184.

Wahl, P., & Weber, G. (1967) *J. Mol. Biol. 30*, 371−382.

Weast, R. C. (1981) *CRC Handbook of Chemistry and Physics*, 60th ed., p D-270, CRC Press, Boca Raton, FL.

Weber, G. (1977) *J. Chem. Phys. 66*, 4081−4091.

Weber, G. (1989) *J. Phys. Chem. 93*, 6069−6073.

Yguerabide, J., Epstein, H. F., & Stryer, L. (1970) *J. Mol. Biol. 51*, 573−590.

BI942225Q